Отпечатано на ротапринте в ИКИ АН СССР

Т - 05382 Подписано к печати 8.04.74

Заказ 2069 Тираж 125 Объем 1,6 уч.-изд.л.

ACADEMY OF SCIENCES OF THE USSR

© INSTITUTE FOR SPACE RESEARCH

Пр - 180

A.I. Gringauz, V.V. Bezrukikh,
T.K. Breus, M.I. Verigin,
G.I. Volkov, A.V. Dyachkov

STUDY OF SOLAR PLASMA NEAR MARS AND ALONG THE PATH EARTH-MARS BY MEANS OF CHARGED PARTICLE TRAPS ON SOVIET SPACECRAFTS, 1971-197?

II. Characteristics of electron component along orbits of artificial satellites of Mars (Mars-2 and Mars-3)

MOSCOW

INSTITUTE FOR SPACE RESEARCH
ACADEMY OF SCIENCES OF THE USSR

Пр - 180

K.I. Gringauz, V.V. Bezrukikh,
T.K. Breus, M.I. Verigin,
G.I. Volkov, A.V. Dyachkov

STUDY OF SOLAR PLASMA NEAR MARS AND ALONG THE PATH EARTH-MARS BY MEANS OF CHARGED PARTICLE TRAPS ON SOVIET SPACECRAFTS, 1971-1973

II. Characteristics of electron component along orbits of artificial satellites of Mars (Mars-2 and Mars-3)

Moscow, 1974

SUMMARY

Results of measurements of characteristics of the solar wind electron component and nearplanet plasma by means of charged particle traps with retarding potentials installed at artificial satellites of the Mars, Mars-2 and Mars-3 are presented. The nearplanet shock wave is detected. Behind the shock wave front the electron density n_e, the temperature T_e substantially increase and electrons with $E \gtrsim 50 \div 70$ ev are observed. The average distance from the Mars surface to the shock wave front is estimated as $\sim$ 2500 km and to the obstacle forming the shock wave - 1400 km. Under the assumption that the obstacle is intrinsic magnetic field of the planet having the dipole character the evaluated value of the magnetic moment of the Mars is 2.4×10^{22} gauss·cm^3. This estimation coincides to the value calculated by Dolginov et all. [29] from the data of magnetic measurements on the same satellites.

I. Introduction

Measurements of solar wind plasma electrons were among the scientific experiments aboard the spacecrafts Mars-2 and Mars-3 launched into orbits around the planet Mars on November 27 and December 2, 1971. On both satellites measurements were perfcrmed by means of identical electron traps.

Preliminary results of these measurements were presented in [1] and [2] . The detailed description of the experiment including the trap's design, the results of laboratory tests of the traps; some characteristics of the electronic and examples of the primary results of measurements were given in [3] .

In this paper characteristics of solar wind plasma electrons obtained during several revolutions of Mars-2, four revolutions of Mars-3 (December 5, 1971 through January 21, 1972*)) and on the route when Mars-3 approached the planet (November 1971) are considered. The method of experimental data processing is discussed.

---

*) After January 21, 1972 the current amplifier of the electron trap aboard the Mars-3 was out of order.

2. Method of data processing

The electron plasma temperature and density were obtained by means of the retarding potential method, i.e. using the electron current dependence on the retarding potential [3] applied to the analysing grid (this dependence is called volt-ampere characteristic or retarding curve).

The recorded collector current is the complicated function of the device parameters and characteristics of the environment medium.

In general the current can depend on electron density n_e electron temperature T_e , electron temperature anisotropy due to interplanetary magnetic field, on the solar wind and vehicle velocities, on electrical potential, on the shape of the spacecraft and its material and so on.

The expression for the collector current of the electron trap is obtained below as function of the plasma electron parameters and the retarding potential; the influence of the spacecraft electrical potential upon the determined solar plasma electron characteristics is evaluated and the influence of photoemission from the spacecraft surface upon the measurements performed evaluated in [3] is specified.

Let us note that the ion part of the collector current can be neglected, because the traps were located on the shadowed part of the spacecraft, i.e. they were in the "ion shadow" (the orientation of electron trap was within an angle not succeeding $\pm 1^0$ in the antisolar direction [3]).

Let us suppose that the uniform electron flow falls on the trap, ϑ - is the angle between its direction and the trap axis, e - the electron charge, v - velocity, dn_e - the electron

concentration in the flux and $S(\vartheta)$ - the aperture area, from which all electrons reach the collector. Then, the collector current is: $dI = dn_e \cdot e \cdot v \cdot \cos(\vartheta) S(\vartheta) \sigma(u)$

where $\sigma(u)$ depends on the retarding potential u .

Using the results of the laboratory study of the trap in the monoenergetic beams [3] we may use the following approximate relation for $\sigma(u)$:

$$\sigma(u) = \begin{cases} 0, & v < \sqrt{\frac{2eu}{\beta m}}; \\ \frac{1}{(\beta-\alpha)}\left(\beta - \frac{2eu}{mv^2}\right), & \sqrt{\frac{2eu}{\beta m}} < v < \sqrt{\frac{2eu}{\alpha m}}; \\ 1, & v > \sqrt{\frac{2eu}{\alpha m}} \end{cases}$$

where $\alpha = 0.95$; $\beta = 1{,}13$ Fig. 5a from [3]).

$S(\vartheta)$ can be found from Fig. 5b in [3] , where the dependence of $\cos(\vartheta) \cdot S(\vartheta) / S(0)$ via ϑ is plotted.

If $f(v, \vartheta, \varphi)$ - is the normalized to unity velocity distribution function in the reference frame related to the spacecraft, then the current, recorded by the trap with the retarding potential u on the electrode will be:

$$I(u) = n_e \cdot e \cdot \int_0^{-\pi/2} \int_0^{\pi} \int_0^{\infty} v \cdot \cos(\vartheta) \cdot S(\vartheta) \cdot \sigma(u) \cdot f(v, \vartheta, \varphi) \cdot v^2 \sin(\vartheta) \cdot dv\, d\vartheta\, d\varphi \qquad (1)$$

According to the solar wind plasma measurements aboard the Vela-4-satellite near the Earth the velocity distribution for electrons (for velocities not being extremely large) may be approximated by the Maxwellian distribution in the frame of reference moving with the bulk velocity of the positive ions [4] .

The electron temperature anisotropy is small [4] (~ 1.1) and is not taken into account in the following calculations. As the bulk velocity of ions ~ 400 km/sed, (directed from the Sun), the vehicle velocity ~ 30 km/sec and the trap axis is directed opposite to the Sun-Mars line direction, the distribution function in the coordinate system related to the trap is taken in the following form :

$$f(v,\vartheta,\varphi)=\left(\frac{m}{2\pi K T_e}\right)^{3/2}\cdot \exp\left\{-\frac{m}{2KT_e}\left[v^2+V^2+2vV\left(\cos\vartheta\cos\delta-\sin\vartheta\sin\delta\cos\varphi\right)\right]\right\} \qquad (2)$$

Here K - is the Boltzman's constant, m - the mass, V - - the electron bulk velocity, taken in the reference frame connected with the vehicle, $\delta \sim 5\text{-}10^{\circ}$ is the angle between the vector $\vec{V}$ and the trap axis, and φ - the azimuthal angle, which is counted off from the vector $\vec{V}$ projection on the plane of the apperture.

Substituting (2) into (1) and integrating by φ we have

$$I(U)=2\pi n_e e\left(\frac{m}{2\pi K T_e}\right)^{3/2}\int_0^{\infty}\int_0^{\pi/2} v^3\sin(\vartheta)\cos(\vartheta)S(\vartheta)\sigma(U)\,e^{-\frac{m}{2KT_e}\left(v^2+V^2-2vV\cos\vartheta\cos\delta\right)} I_0\left(\frac{mvV}{KT_e}\sin\vartheta\sin\delta\right)dv\,d\vartheta \qquad (3)$$

where I_0 - is the modified Bessel function.

We can rewrite (3) in the form:

$$I(U)=A\cdot n_e\sqrt{T_e}\,\Psi\left(\frac{mV^2}{2KT_e},U\right),$$

where A = const. If U = 0 and V and T_e are typical values for the solar wind, then $\Psi\left(\frac{mV^2}{2KT_e},0\right)$ is approximately equal to unity and the current, corresponding to the zero retarding potential

$$I_{max}\sim A\cdot n_e\sqrt{T_e} \qquad (4),$$

i.e. it depends on the plasma electron flux from the space (proportional to $n_e\sqrt{T_e}$) and mainly on its density n_e.

The theoretical retarding curve for the electron trap was calculated by means of computer using the expression (3).

The retarding curve normalized to unity for U = 0 V and four values of bulk velocities: V = 0, 300, 450 and 600 km/sec, T_e = 10 ev and δ = 0° is presented in Fig. 1. It can be shown, that the bulk velocity variation from 300 to 600 km/sec may give the temperature estimation error of the order of 5%, if the retarding curve for = 450 km/sec is used for electron temperature determinations. While the bulk velocity rises, the retarding curve is becoming stronger dependent on the angle between the trap axis and the bulk velocity vector, but when it reaches 600 km/sec the difference in characteristics, calculated for δ = 0 and δ = 10° is only ~ 1,5%.

The volt-ampere characteristics recorded onboard the Mars-3 at different moments are given in Fig. 2 by crosses. Smooth curves present volt-ampere characteristics of the trap, calculated numerically from (3) for V = 450 km/sec; the electron temperatures and densities are shown on the same figure. The theoretical curves fitting to the experimental points were found by means of the least-square fitting [5].

Let us consider the satellite electrical potential influence upon the accuracy of electron temperature determinations.

The thermal velocity of the solar wind plasma electrons $\bar{v}$ corresponding to the temperature $T_e \sim 10^5$°K is $\bar{v}=\sqrt{\frac{2KT_e}{m}}$ ~ 1700 km/sec and is about 3-5 times greater

than the electron bulk velocity.

Thus for some evaluations one can neglect the movement of the spacecraft.

The Debay radius $D = \sqrt{\frac{\kappa T_e}{4\pi n_e e^2}} \sim 10$ m in the undisturbed plasma with the electron density $n_e \sim 5$ cm^{-3}.

The electric field in the neigbourhood of the spacecraft is the Columb type since R - the characteristic size of the spacecraft is smaller than D. (The spacecraft is supposed to be the sphere of radius R).

If the electric potential of the surface φ_0 ($\varphi_0 \ll \frac{\kappa T_e D}{e R} \sim$ ~ 50-60 V) is assumed to be small, then at the distance from the center of the spacecraft $r > D$, the electric field is weak ($\varphi \sim \varphi_0 (\frac{R}{r}) \ll \frac{\kappa T_e}{e}$) and it doesn't substantially disturb the particles motion [6]. One can show, that in such a case the electron distribution function near the satellite surface can be presented by the following expression:

$$f(v, \vartheta, \varphi) = \begin{cases} \left(\frac{m}{2\pi \kappa T_e}\right)^{3/2} e^{\frac{e\varphi_0}{\kappa T_e}} e^{-\frac{m v^2}{2\kappa T_e}}, & v > \sqrt{\frac{2e\varphi_0}{m}}; \\ 0, & v < \sqrt{\frac{2e\varphi_0}{m}} \end{cases}$$

We suppose that the electron distribution when $r \to \infty$ is Maxwelian and the satellite electric potential is positive.

If the satellite surface potential is negative there would appear the factor $exp\left(-\frac{e|\varphi_0|}{\kappa T_e}\right)$ in the distribution function. Substituting this velocity distribution into expression (1) and performing the integration, we find the result, shown in the Fig. 3. One can see that the current when the satellite body potential is positive and the retarding potential on the

grid $u > \beta \varphi_0$ the collector current increases by factor $exp\left(\frac{e\varphi_0}{\kappa T_e}\right)$ and hence the form of vol-ampere characteristic in a semilogarithmic scale doesn't change.

The current, collected by the trap, when retarding potential on the grid $u < \alpha \varphi_0$ doesn't depend on a voltage and exceeds the current corresponding to $\varphi_0 = 0$ and $u = 0$ by factor of $\left(1 + \frac{e\varphi_0}{\kappa T_e}\right)$. The trap current the satellite body potential being negative, decreases by factor of $exp\left(-\frac{e|\varphi_0|}{\kappa T_e}\right)$. As a result we can conclude that if the electron temperature is estimated by using that part of the volt-ampere characteristic which corresponds to $u > \beta \varphi_0$, then in such an approximation this estimation doesn't depend on potential.

From [3] it follows that for retarding potentials exceeding 10 V the influence of the photoemission upon volt-ampere characteristic is negligible.

The analysis of data, obtained from Mars-3 had shown that the retarding curves calculated with the use of experimental points, corresponding to retarding potentials exceeding 10 V quite well describe the experimental retarding curves up to the retarding potential 4-6 V.

It means that the satellite electric potential doesn't obviously exceed several volts otherwise there would be observed a break in the volt-ampere characteristic at the point, corresponding to the satellite potential (Fig. 3). If the satellite potential is of the order of several volts, the photoelectrons with energies exceeding several ev will not return to the satellite surface. Thus for temperature estimation we can neglect the photocurrent effect beginning from the point which corresponds to the retarding potential 4-6 V.

The electron density estimations are less reliable than

the corresponding temperature estimations since the first are much more influenced by the satellite potential, the variations of bulk velocity and by the difference of the real trap grid system transparency from the used in calculations optical one.

The electron concentration n_e was found in assumption that the satellite potential $\varphi_0 = 0$ and the electron bulk velocity $V \sim 450$ km/sec. If the bulk velocity changes from 300 km/sec to 600 km/sec the electron density estimation may correspondingly be either overstated or understated in ~1,3 times. The positive satellite body potential leads to the $e^{\frac{e\varphi_0}{\kappa T_e}}$ overestimation of n_e, i.e. the calculated value of n_e may exceed 1,5–2 times the real one if the positive satellite potential is of the order of several volts.

2. Experimental results and their interpretation

As have been already noted in this paper are presented the data from electron traps onboard the satellites Mars-2 and -3 during the period from November 1971 till January, 1972. One of the orbits of the Mars-2 and the evolution the Mars-3 orbits during the first four revolutions are shown in Fig. 4 in a polar reference frame, where the abscis axis coincides with the Sun–Mars-line, while the polar angle is the Sun-Mars-Satellite angle. Mars-2 has the orbit with the pericentre ~ 1300 km, apocentre ~ 28000 km and the revolution period ~ $17^h5\frac{1}{2}^m$. The pericentre and apocentre of the Mars-3 satellite are correspondingly ~1100 km and ~212000 km and the revolution period ~ $12^d16^h30^m$.

The variations of the retarding curves and, consequently, of the electron characteristics for the first four revolutions of the Mars-3 around the planet which are shown in Fig. 4 appeared to be roughly similar and repetitive. All the orbit

were subdivided into four zones which corresponded to different shapes of the retarding curves. These zones marked by different shadings and letters are shown in Fig. 4 for the second revolution of the Mars-3 (from 12 to 25 of December, 1971).

Zone A corresponds to the descending part of the orbit, Zone B – to the pericentre region of the orbit, Zone C – to the ascending part and Zone D – to the apocentre part of the orbit. The examples of retarding curves typical for these four zones are shown in Fig. 5.

One can see from Fig. 5 that the general shape of the retarding curves has considerably changed along Mars-3 orbit during the satellite revolution; in particular the values of I_{max} and the retarding potentials on the analysing grids of the traps. E_T corresponding to the bend of electron registration were changing in wide limits.

It was shown above (see the expression (4), that I_{max} is in general determined by the solar wind electron density n_e (if photoelectrons are not taken into account). In reality the photoelectrons from the illuminated part of the satellite surface and the secondary electrons [3] give a certain contribution into I_{max}. It must be pointed out, however, that the observed considerable variations of I_{max} (up to the order of value) can't be related to variations of the photoemission, because the satellite orientation relatively to the Sun during the described measurements remained constant and the intensity of that part of solar radiation spectrum, which is responsible for the photoemission is rather stable [9].

The increase of T_e leads naturally to the rise of E_T however, the main cause of E_T – increase is the increase

of flux intencities of "superthermal electrons" (which correspond to "superthermal tails" of the velocity distribution function). These electrons are observed by sensitive instruments on board the Earth Vela-type Satellites [4, I0] , in the undisturbed solar wind and in the magnetosheath behind the shock wave front. The appearance of electrons with energies > 50--100 ev served as an indication that the satellite OGO-5 crossed the shock wave front [II] .

Thus, the variations of I_{max} and E_T , which are accessible directly from retarding curves even without their further processing rather obviously characterise the satellite plasma environment.

That is why we present the variations of I_{max} and E_T along the Mars-3 orbit in Fig. 6-9. The electron density n_e and temperature T_e , calculated with help of the above described method, are also plotted in these Figures. The lower curves in these Figures give the K_p -indexes, characterizing the magnetic field disturbances at the Earth (these curves will be used further for the interpretation of results).

Letters p and a mark the pericentre and apocentre of orbits while letters A, B, C and D the conventional orbit zones.

Let us consider the peculiarities of each of these zones. Though the phenomena observed in each zones for different revolutions of the Mars-3, had definite similarities, they also possessed some distinctions.

In Zone A the electrons are completely retarded at potentials $\sim$ 30-40 V and the measured currents I_{max} are relatively small. The electron concentration and temperature vary

within the limits of 3÷6 cm^{-3} and $(60 \div 100) \cdot 10^{3o}K$ respectively. The shape of retarding curves approach the calculated one, which means that the maxwellian distribution of electrons takes place. The "superthermal" electrons, responsible for the "tails" in the retarding curves (which were observed in the undistrubed solar wind near the Earth's orbit by Montgomery et al. [4]), were not registered within the trap sensitivity limits. However, during the fourth revolution of the Mars-3 on January 12, 1972 (Fig. 9) disturbance was observed in Zone A, which led to a drastic increase of I_{max} and E_T (the section with small slope appeared in the retarding curve, which corresponded to the "superthermal tails"). The temperature and electron density also increased up to $\sim 200 \cdot 10^{3o}K$ and ~ 12 cm^{-3} respectively.

The retarding curves, corresponding to the ascending parts of the orbits (Zone C) were similar to the retarding curves of Zone A but differed from the last by somewhat higher values of I_{max}; T_e and n_e also exceeded the values, which were typical for zone A and were $(90 \div 140) \cdot 10^{3o}K$ and 4÷6 cm^{-3}. The "superthermal tails" were observed in Zone C during the second revolution.

When the Mars-3 approached the apocentres on the ascending parts of its orbit. (Zone D) there were registered the increases of I_{max} up to the order of value, of E_T up to 150-270 v, of T_e up to $300 \times 10^{3o}K$ and of n_e up to 20 cm^{-3}. These disturbances during the third revolution were slowly expressed.

In Zone B disturbances, characterized by the sharp increase (during the time interval between two successive measurements) of the analysed parameters were also observed.

For the first revolution (Fig. 6) data corresponding to the regio. near the pericentre are absent, during the seco.t--fourth revolutions plasma traps and magnetometers were switched off near the pericentre, and only on January 21 the plasma measurements were performed near the pericentre.

The alterations of the shape of volt-ampere characteristics observed during several hours in pericentre region on January 21 1972 are shown in Fig. 10a. The variations of the tra. current for four fixed values of the retarding potential during the same time-interval are shown in Fig. 10b.

One can see, that in the time interval, noted by the solid line, parallel to the time axis, the shape of retarding curves is distorted, T_e and n_e increase and energetic electrons appear. It is very difficult to estimate correctly T_e and n_e using these distorted volt-ampere characteristics When it appeared possible to do this, it was found ut that T_e had increased up to $(200\div300)\cdot10^{3o}$K and n_e up to ~ 20 cm^{-3}. The disturbances in Zone B may be identified with the shock wave, created by the interaction of the solar wind with the planet and they will be discussed in more detail below.

In A, C and D zones electron trap apparently registered the solar wind at the orbit of Mars undisturbed by the planet. In such a case disturbances observed far from the planet can be accounted for by changes of the solar wind characteristics. Let us compare variations of Kp-indexes as determined from ground station observations and solar wind parameters as measured at the Earth's orbit on Vela satellites [7] with variations of parameters of the electron plasma at the Mars orbit during the period under consideration.

During fourth revolution there observed two disturbances far from the planet (January, 13-14 and 19-20). In periods January, 15-19 and 21-29 magnetic storms were registered by ground stations (fig. 9). In the same periods values of the solar wind velocity and density considerably increased as measured by Vela-3 from 350 km/sec and 5 cm^{-3} to 600-700 km/sec and 20 cm^{-3} [7] . In this period intensive solar flares were also observed. When comparing these events the time delay due to mutual locations of the Mars, the Earth and the Sun should be taken into account. In January, 1972 the Mars laged behind the Earth in azimuth of rotation by $\Delta\alpha \sim 50\text{-}65^\circ$ and was located $\Delta R \sim$ ~70-75 millions km farther from the Sun than the Earth. The time delay of the events may be evaluated from the following relation [8] :

$$\Delta t = -\frac{\Delta R}{V_R} + \frac{\Delta\alpha}{\Omega}$$

when $\Omega \simeq \pm 13.3^\circ$/day - the angular velocity of the solar rotation, V_R - the radial velocity of a disturbance in the solar wind. At $V_R \approx 300\text{-}500$ km/sec the values of Δt was ~2-3 days; on the Mars solar wind disturbances should be observed earlier than on the Earth. Therefore one can conclude that January 15 and 21 disturbances were observed on the Earth, which were registered at the Mars orbit on January, 13 and 19.

We has no success in establishing of relation between phenomena observed near the Mars and near the Earth during the first and third revolutions of the spacecraft Mars-3 (see fig. 6 and8). In these periods there were not observed an peculiarities on the Earth: K_p -index increased up to 4 very seldom, its average value was 0-1. The third revolution of Mars-3 was characterized by monotonous weak disturbances with

less increases of I_{max} and E_T near the pericentre compared to other revolutions. On the first revolution near the apocenter the shorttime large disturbance was observed which was not followed by a magnetic storm on the Earth.

During the second revolution of "Mars-3" (fig. 5, 7) on 16 December at ~21^{h}00^m the strong magnetic storm began on the Earth. At this time the maximum K_p-index reached 7. The disturbance lasted to December 19. Corresponding disturbances of the solar wind at the Mars orbit should been observed approximately two days earlier. Indeed, on 14 December after 23.00 values of I_{max} in volt-ampere characteristics, registered by "Mars-3" slightly increased and superthermal tails appeared. The magnetic storm lasted to December, 20, the maximum amplitude was registered on 18 December (on 15 December at ~ 05^{h}30^m the nearplanet shock wave was observed on the ground of this disturbance).

Disturbances in the solar wind similar to abovementioned ones were observed in November 1971 on "Mars-3" when the spacecraft was in the solar wind undisturbed by the planet (fig. 11).

The data of simultaneous measurements on Mars-2 and Mars-3 during the second revolution of Mars-3 (fig. 7 and 12) also show that variations of the electron plasma component detected far from the planet reflect variations of the solar wind. From fig. 7 and 12 one can see that on 18 December disturbances of the solar wind were simultaneously registered on both spacecrafts and during the quiet period, on 22-23 December, values of I_{max} and E_T considerably decreased on both spacecrafts. In this period Mars-2 did not move away from the planet more than by 28000 km, and Mars-3 was at the distance > 150000 km.

Simultaneous registration of the appearance and disappearance of disturbances on both spacecrafts located in different regions of interplanetary space shows that observed variations reflected variations of "the solar wind weather".

According to magnetohydrodynamical theory five types of discontinuities can be observed in the solar wind: tangential, contact, rotational and shock wave discontinuities (rapid and slow shock waves) [22] . During disturbances registered far from the planet an increase of the temperature, density (see fig. 7, 9, 11) and magnetic field*) (fig. 13) simultaneously occured. This allows to suggest that observed disturbances correspond to interplanetary shock waves. Really in case of rotational discontinuities a temperature and density should not vary, in case of contact discontinuities an increase of a density should be accompanied by a decrease of a temperature and in the case of tangential discontinuities an increase of a temperature and density should be accompanied by a decrease of a magnetic field [22] . In a near-planet shock wave simultaneous variations of solar wind parameters are also observed.

Let us now return to the consideration of the interaction of the solar wind with the planet Mars. The interaction of the solar wind with the Earth is known fairly well (see, for example, [10, 11, 22, 23]). The shock wave front, the magnetosheath and the magnetopause were observed by means of magnetometers and plasma probes on many spacecrafts. Experimental data on the

---

*) The data of simultaneous measurements of the magnetic field on 18 December 1971 during a disturbance were kindly given us by Sh.Sh. Dolginov, Ye.G. Yeroshenko, L.N. Zhuzgov.

solar wind near other planets are yet not numerous.

The disturbance of the solar wind by the planet (intrinsic magnetic field of Venus was not revealed) was observed on 18 October, 1967 by means of plasma traps and magnetometers on the spacecraft Venera-4 [12, 13] , on 19 October, 1967 on the spacecraft Mariner-5 [14] and on 17 June, 1969 by means of plasma traps on the spacecraft Venera-5 [15] . Near the Mars up to 1971 the only experiment was performed on the Mariner-4 in which a weak disturbance of the interplanetary magnetic field was registered at the distance $\sim 1.5 \cdot 10^3$ km from the Mars on the single pass of Mariner-4 [16] . Although this disturbance of the magnetic field might be accounted for by some processes in the solar wind which were not related to the planet (such interplanetary shock waves are frequently observed in the solar wind) it was interpreted as the crossing of the near-Martian shock wave front by the spacecraft. The origins of this near-Martian shock wave were repeatedly discussed afterwards in different theoretical papers [17] . It was suggested that an obstacle formed either by own magnetic field of the Mars (value of its magnetic moment is $\sim 1.7 \cdot 10^{22}$ gauss$\cdot$cm^3 [16] or by the ionosphere [18, 19, 20, 21] can cause the shock wave near the Mars. In the latter case were considered the direct interaction of the solar wind with the ionosphere (with taking into account of photochemistry, charge exchange processes and others) [20] , or the tangential discontinuity between the solar wind plasma and the planet ionosphere [19] , or so-called magnetic barrier [21] .

The location of the shock wave front depends on dimensions of the obstacle. Therefore the experimental determination of

the shock wave front location near the planet allows to evaluate dimensions of the obstacle and exclude some of above-mentioned hypotheses predicting obstacle dimensions, which contradict to experimental data.

In [2] the preliminary results of estimations of the obstacle dimensions were presented from shock wave front locations according to the data of electron traps aboard the Mars-2 and Mars-3. These estimations were made under the assumption of sphericity of the obstacle using simple gazodynamical relations [24] . It was obtained that the average radius of the obstacle was ~ 4500 km and the average areocentrical distance to the bow shock-stagnation point was ~ 5500 km.

Below obstacle dimensions are estimated in accordance with calculations of the shock wave front location [22] under the assumption that the obstacle has the form of a stretched body of revolution similar to the Earth's magnetosphere. In fig. 14 parts of orbits of Mars-2 and Mars-3 are shown in which the spacecrafts crossed the shock wave front. The criterion of the crossing of the near-Martian shock wave front as well as in number of cases for near-Earth shock wave [4, 10, 11] was the appearance of "superthermal" electrons and the abrupt increase of parameters (n_e , T_e , I_{max}). Retarding curves obtained at near-planet points of these parts of orbits (fig. 14) are typical for the magnetosheath, and those obtained at the most distant points - for the undisturbed solar wind. The direction of pointers corresponds to that of satellite motion and the lengths of parts of orbits depend on the instrument operation regime. On 8 January, 21 January and 12 May, 1972 measurements were made every 2 min, on 15 December, 1971, 9 January, 1971 - every 10 min.,

and on 17 December, 1971 - every 20 min (see [3]). The solid line shows the form and dimensions of the obstacle, the dashed line - the shock wave front location for Mach number $M_\infty \cong 8$ [25] and $\gamma = 5/3$ [22]. Obstacle dimensions are chosen in such a way that the sum of the square of the distance was minimum from both ends of parts of trajectories (fig.14) to the shock wave front formed by this obstacle. The areocentric distance to the stagnation point of the obstacle is ~4800 km and to the stagnation point of the shock wave front - 5900 km (~1400 km and ~2500 km from the Mars surface respectively). Both values of distances are somewhat more than in [2]. The obtained size of the obstacle does not agree with hypotheses [18, 19, 20].

According to these hypotheses the Martian ionosphere is the obstacle. In [19] dimensions of the obstacle is determined by the balance of the solar winddynamical pressure and the ionospheric charged particle pressure (i.e. the boundary lies at the height ~170 km). In [20] it is suggested that the thermalized solar wind is decelerated at the height of 100-200 km above the Mars surface. Really the experimental data on the electron concentration distribution in the Martian ionosphere, obtained from the radio occultation observations eclipses of the same spacerafts Mars-2 [26] and Mariner-9 [27, 28], show that the maximum of the ionospheric electron density is located at the height ~140 km and at ~300-350 km the Martian ionosphere pressure approximately two orders less than the solar wind dynamical pressure at the Mars orbit. However, results of our measurements may be easy explained under the assumption that the obstacle forming the shock wave is the magnetic field. If the Mars has intrinsic magnetic field and the magnetosphere, the value of the magnetic moment of the Mars may be estimated from following expression [22]:

$$M_M = D^3\sqrt{2\pi K \rho_\infty V_\infty^2},$$

where

$K = 0.88$, ρ_∞ and V_∞ -density and velocity of the solar wind respectively, D -areocentric distance to nosing point of the magnetosphere. The value of D = 4800 km (see dimension of the obstacle estimated above) corresponds to the density of 3 cm^{-3}, velocity of $V_\infty \sim 450$ km/sec and magnetic moment of the Mars $M_M = 2.4 \times 10^{22}$ gauss·cm^3. Magnetic measurements conducted simultaneously with ours on the same satellites [29] allowed to conclude the Mars can have own dipole magnetic field. The value of the magnetic moment determined in [29] agrees to our estimations. Estimations of M_M made in [16] according to the data from Mariner-4 do not contrast with our estimations either.

Results of simultaneous measurements of plasma characteristics and the magnetic field from satellites Mars-2 and Mars-3 and the comparison of these results with similar measurements near the Earth and the Venus can serve as the confirmation of the hypothesis on the existing Martian intrinsic magnetic field [29].

Fig. 15 shows three components of the magnetic field taken from [29], values of electron trap currents at zero retarding potential (I_{max}) and electron temperatures (T_e) obtained on 21 January, 1972 (see fig. 9) in the region of pericentre. One can see from this figure that at moments of time corresponding to abrupt increases (or decreases) of I_{max} and T_e (Mars-3 crossed the shock wave front) the magnetometer also registered

increases (or decreases) of the magnetic field and the level of its fluctuations. In fig. 15 these moments are marked by figures 1 and 4. In accordance with [29] the boundary of a hypothetical Martian magnetosphere is marked by figures 2 and 3. At the moment 2 the value of the magnetic field abruptly increased and up to the moment 3 it remained high compared to those in the magnetosheath. In the same interval 2-3 the value of I_{max} (which is mainly determined by the electron flux) had substantially less average values than in the magnetosheath (intervals of time 1-2 and 3-4).

As it is known simultaneous measurements of plasma characteristics and the magnetic field were conducted in the environs of the Earth and the Venus. Intrinsic Venusian magnetic field either is absent, or is very small [13] therefore the behaviour of the plasma and the magnetic field as the satellite approaches the Venus after the crossing of the shock wave front differs from that near the Earth.

When approaching the Earth a satellite crosses the magnetopause and enters the magnetosphere. At this moment the magnetic field increases and becomes regular and the density n_e and charged particle flux N drops (in the magnetosheath n_e is considerably higher than in the boundary layer inside the magnetosphere [30, 31, 32]). Near the Venus a quite different plasma behavior is observed: during the spacecraft Venera-4 approach to the planet, the values of $|B|$ and N varied practically synchronous at a distance of $\sim 20 \times 10^3$ km up to the end of measurements at the height $\sim$ 300 km [12] .

It is easy to see that simultaneous variations of the plasma and magnetic field near the Mars are more like similar variations in the near-Earth environs than in near-Venus one. The authors of the present paper suppose that fig. 15 confirms the correctness of the hypothesis on Martian intrinsic magnetic field and Martian magnetosphere as the obstacle forming near-planet shock wave. The joint consideration of simultaneous measurements of characteristics of the electron plasma and the magnetic field for a number of passes of the satellites near the planet will be conducted in future.

Conclusions

Results of measurements of the solar wind electron plasma characteristics allowed to make following conclusions:

1. The electron temperature and the density of the undisturbed or slightly disturbed solar wind of the Mars orbit during the period of measurements were $(60 \div 120) \times 10^{3^o}$K and 3÷6 cm^{-3} respectively.

2. The shock wave is detected which is formed by the interaction of the solar wind with the planet. With using in Mach number $M_\infty = 8$, the estimation of the distance from the planet surface to the shock wave front at the stagnation point $\sim 0.7 R_M$.

3. The crossing of the near-planet shock wave front by the Mars-2 and Mars-3 corresponds to the substantial increase of the electron temperature (up to $200 \div 300 \times 10^{3^o}$K), the density (up to ~ 20 cm^{-3}) and to the appearance of energetic electrons with $E_r > 50 \div 70$ ev.

4. Near the planet and far from the planet ($80 \div 100 \times 10^3$km) at orbit of the artificial satellite of the Mars the interplanetary shock-waves were detected.

5. The abrupt increase of T_e up to $300\ 10^{3^o}$K, n_e up to

20 cm^{-3} and the appearance of "superthermal" electrons with $E_T > 150 \div 270$ ev were observed in the interplanetary shock waves.

The appearances of these disturbances are correlated with the magnetic disturbances and magnetic storms observed at the Earth.

6. The comparison of measurements of the solar wind electron component and the magnetic field from the satellite Mars-2 and Mars-3 showed that the substantional increases of T_e, n_e and the appearance of "superthermal" electrons were simultaneous with substantial increases of the magnetic field and the level of its fluctuations in the near-planet and interplanetary shock waves.

7. The location of the near-Martian shock wave front determined from measurements of the plasma electron component and the comparison of variations of the plasma and the magnetic field near the Mars, the Earth and the Venus allow to conclude that Martian intrinsic magnetic field with $M_M \sim 2{,}4 \times 10^{22}$ gauss$\cdot cm^{-3}$ may be the cause of the near-Martian shock wave. Thus evaluation of M_M agrees to the value of M_M calculated from the data of magnetic measurements presented in [29].

Figure captions

Fig. 1 Calculated normalized volt-ampere characteristics of the electron trap at different values of the bulk velocity.

Fig. 2 Experimental and calculated volt-ampere characteristics of the electron trap.

Fig. 3 The influence of the spacecraft potential on the volt-ampere characteristics of the electron trap.

Fig. 4 Orbits of the artificial satellites of the Mars.

Fig. 5 Volt-ampere characteristics typical to different zones.

Fig. 6 Variations of values of I_{max} and E_T during the first revolution of Mars-3 and simultaneous variations of K_p -indexes recorded on the Earth.

Fig. 7 Variations of parameters of the plasma electron component during the second revolution of Mars-3 and simultaneous variations of K_p-indexes recorded on the Earth.

Fig. 8 Variations of parameters of the plasma electron component during the third revolution of Mars-3 and simultaneous variations of K_p -indexes recorded on the Earth.

Fig. 9 Variations of parameters of the plasma electron component during fourth revolution of Mars-3 and simultaneous variations of K_p-indexes recorded on the Earth.

Fig. 10. a) The change of the form of volt-ampere characteristics in the pericentre region of Mars-3;

b) Values of currents corresponding to four values of the retarding potential in the pericentre region of Mars-3

Fig. 11 Variations of parameters of the plasma electron component along the path of Mars-3 in November, 1971.

Fig. 12 Variations of values of I_{max} and E_T recorded on Mars-2 in December, 1971

Fig. 13 Simultaneous changes of values of I_{max}, T_e and the magnetic field far from the planet.

Fig. 14 Parts of Mars-2 and Mars-3 orbits in which the crossing of the shock wave front was detected.

Fig. 15 Simultaneous measurements of parameters of the plasma electron component and the magnetic field in the pericentre region.

I. K.I. Gringauz, V.V. Bezrukikh, G.I. Volkov, T.K. Breus, L.S. Musatov, L.P. Havkin, G.F. Sloutchenkov. Icarus, 18, 54, 1973

2. K.I. Gringauz, V.V. Bezrukikh, G.I. Volkov, T.K. Breus, L.S. Musatov, L.P. Havkin, G.F. Sloutchenkov. J. Geoph.Res., 78, 5808, 1973

3. К.И.Гringауз, В.В.Безруких, Г.И.Волков, М.И.Веригин, Л.Н.Давитаев и др. Исследование солнечной плазмы вблизи Марса и на трассе Земля-Марс при помощи ловушек заряженных частиц на советских космических аппаратах 1971-1973 гг. Космич.исслед., 1974.

4. M.D. Montgomery, S.J. Bame, A.J. Hundhauzen. J. Geoph.Res., 73, 4999, 1968

5. Д.Худсон. Статистика для физиков, М., "Мир", 1967, 196.

6. А.В.Гуревич, Л.П.Питаевский, В.В.Смирнова, УФН, 99, 3, 1969.

7. Solar Geoph. Data (Comprehensive report), U.S. Department of Commerce Publ., May, June, July, 1973

8. P.J. Coleman, Jr., E.J. Smith, L. Davis, Jr., D.E. Jones, 74, 2826, 1969

9. D.F. Heath, J. Geoph. Res., 78, 2779, 1973

10. M.D. Montgomery, J.E. Asbridge, S.I. Bame, J. Geoph. Res., 75, 1217, 1970

11. M. Neugebauer, C.T. Russell, J.V. Olson. J. Geoph. Res., 76, 4366, 1971

12. К.И.Гringауз, В.В.Безруких, Л.С.Мусатов, Т.К.Breус. Космич. исслед., 6, вып.3, 411, 1968.

13. Ш.Ш.Долгинов, Л.Н.Жузгов, Е.Г.Ерошенко, Космич.исслед., 6, № 4, 1968.

14. H.S. Bridge, A.J. Lazarus, S.W. Snyder, E.J. Smith, L.Davis Jr., P.J.Coleman, Jr., D.E.Jones, Science, 158, 1669, 1967

15. К.И.Гringауз, В.В.Безруких, Г.И.Волков, Л.С.Мусатов, Т.К.Breус. Космич.исслед., 8, № 3, 431, 1970.

16. M.Dryer, G.P.Heckman. Solar Phys., 2, 112, 1967

17. F.S.Michel. Rev. of Geoph. and Sp.Phys., 9, 2, 1971

18. A.J. Dessler, in "The atmosphere of Venus and Mars", ed. by J.C.Brandt, M.B.McElroy. New York, London, Paris, 1968, 1968, p. 241

19. J.K. Spreiter, A.L. Summers, A.W. Ricci. Pl.Sp Sci., 18, 281, 1970

20. P.A. Cloutier, M.B.McElroy, F.C.Michel. J.Geoph.Res., 74, 6215, 1969.

21. F.S.Johnson, J.E.Midgley, Sp.Res.IX, 760, 1969.

22. Дж.Р.Спрайтер, А.И.Аликсне, в кн."Физика магнитосферы", Мир, 1972, стр.19.

23. J.H. Wolfe, D.S.Intrilligator, Sp.Sci.Rev., 10, 511, 1970

24. T.Obayashi, J. Geoph.Res., 69, 861, 1964

25. M. Dryer, Cosmic Electrod., 1, 115, 1970.

26. М.А.Колесов, Н.А.Савич, Радиотехника и электроника, 1973, № 10 (в печати).

27. A.J. Kliore, G.Fjeldbo, B.L. Seidel, D.L. Cain, M.J.Synes, S.I. Rasool. Icarus, 17, 484, 1972

28. A.J. Kliore, G. Fjeldbo, B.L. Seidel, M.J.Synes, P.M.Woiseshyn. Science, 175, 313, 1972

29. Ш.Ш.Долгинов, Е.Г.Ерошенко, Л.Н.Жузгов, ДАН СССР, 207, 1296, 1972.

30. K.I. Gringauz, G.N. Zastenker, M.Z. Khokhlov. Variations of magnetopause location according to charged trap particle data from satellites "Prognoz" and "Prognoz-2", preprint, Report to IAGA Symposium, Kyoto, Japan, 1973.

31. E.W. Hones, Jr. Magnetospheric plasma flow and the nature of the magnetospheric boundary layer, preprint LA-UR 73--732 Los Alamos Scientific Laboratory of the University of California, 1973.

32. J.H. Wolfe, D.D.McKibbin, in "Physics of the Magnetosphere", ed. by R.H. Carovillano, J.F.McClay, H.R. Radoski, D.Reidel Publ. Co., Dordrecht-Holland.

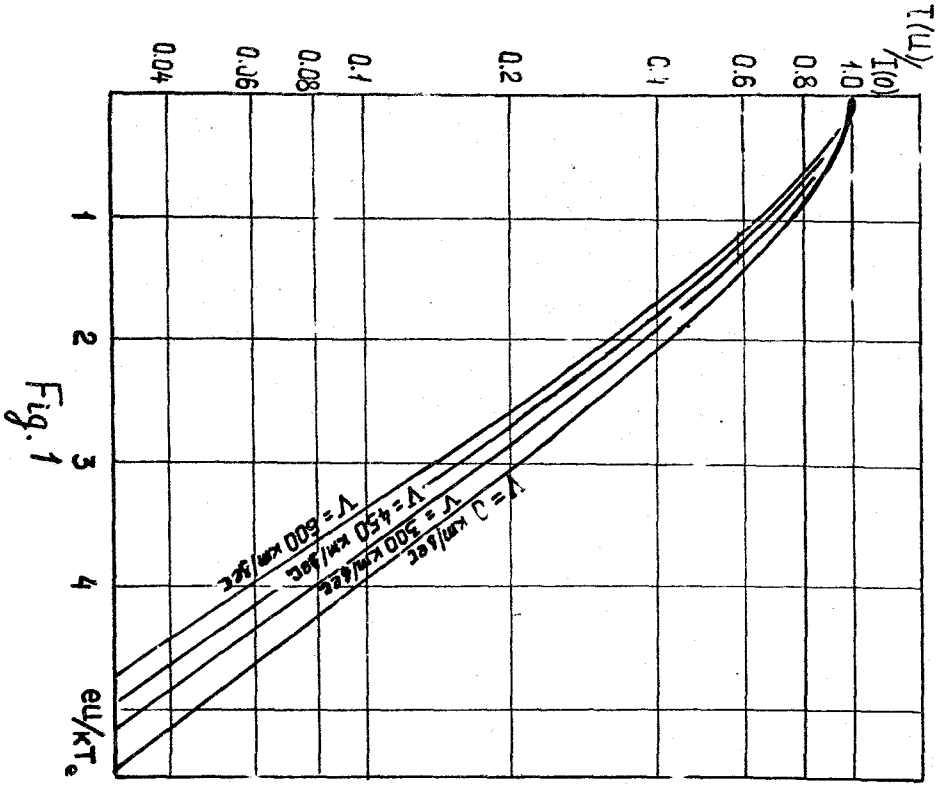
T(U)/T(0)
0.04
0.06
0.08
0.1
0.2
0.4
0.6
0.8
1.0
1
2
3
4
eU/kT_e
V = 600 km/sec
V = 450 km/sec
V = 300 km/sec
V = 0 km/sec

Fig. 1

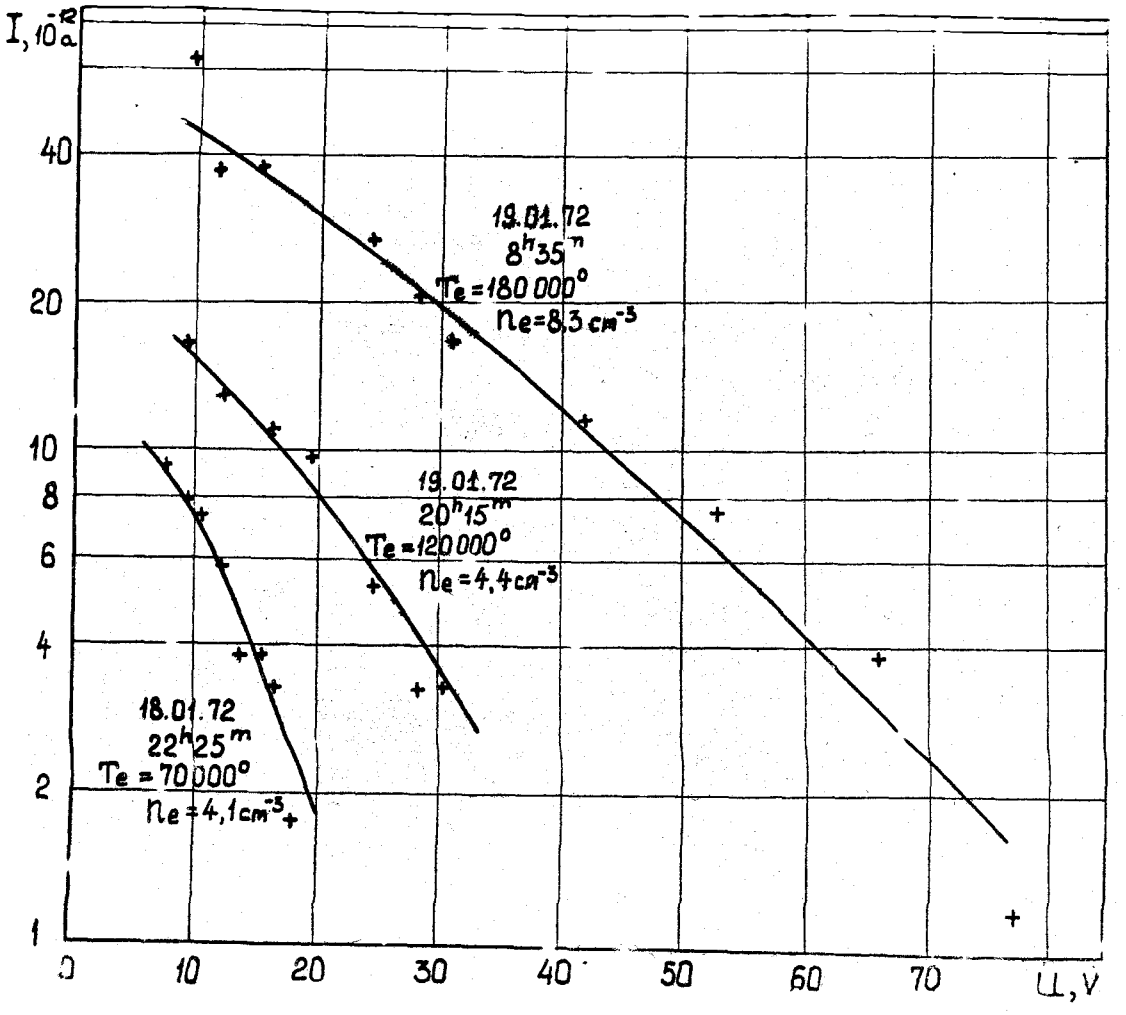
I, 10^-12 A
40
20
10
8
6
4
2
1
19.01.72
8h35m
Te = 180 000°
ne = 8,3 cm^-3
19.01.72
20h15m
Te = 120 000°
ne = 4,4 cm^-3
18.01.72
22h25m
Te = 70 000°
ne = 4,1 cm^-3
0
10
20
30
40
50
60
70
U, V

Fig 2

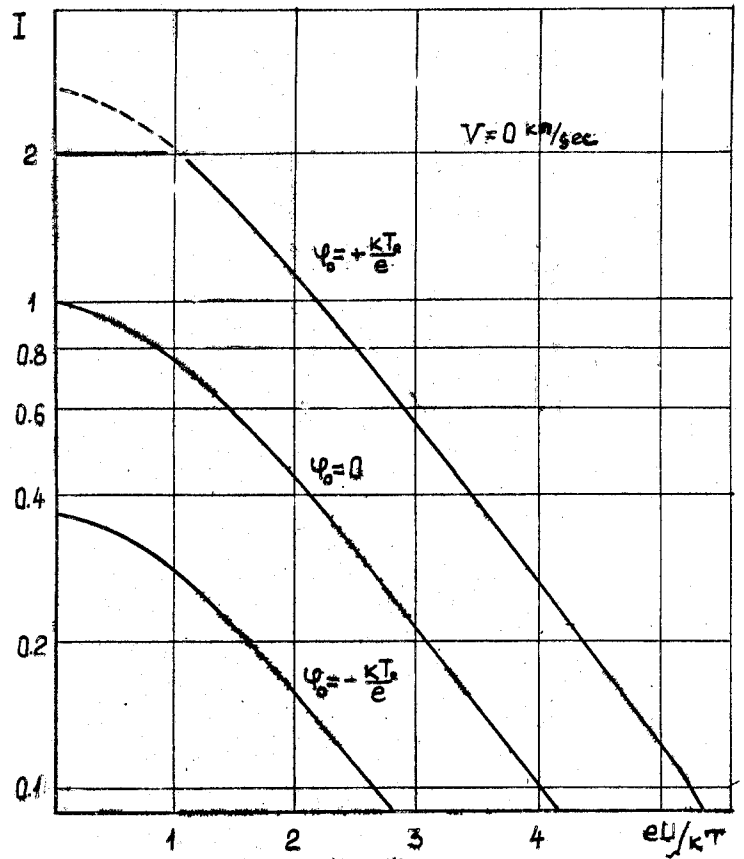

Fig 3

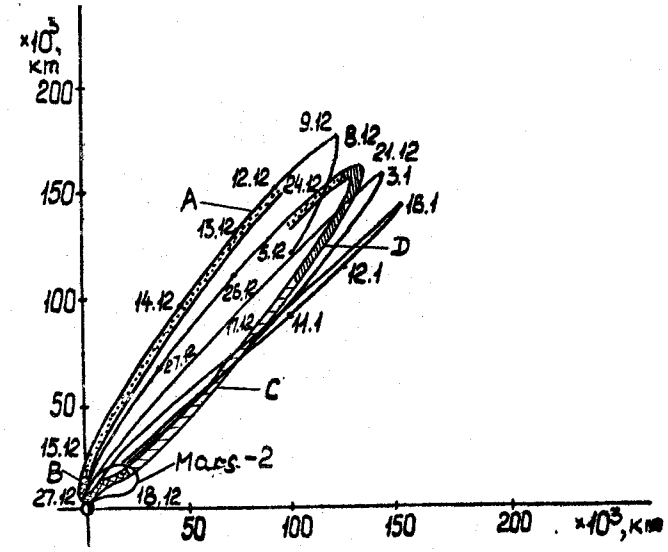

Fig 4

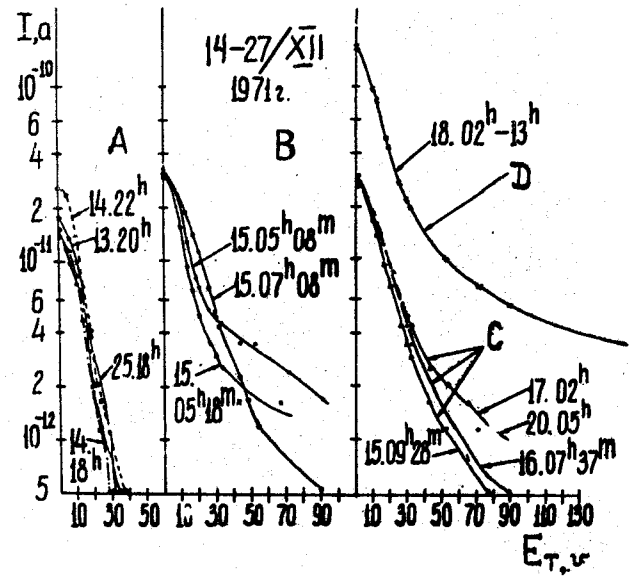

Fig. 5

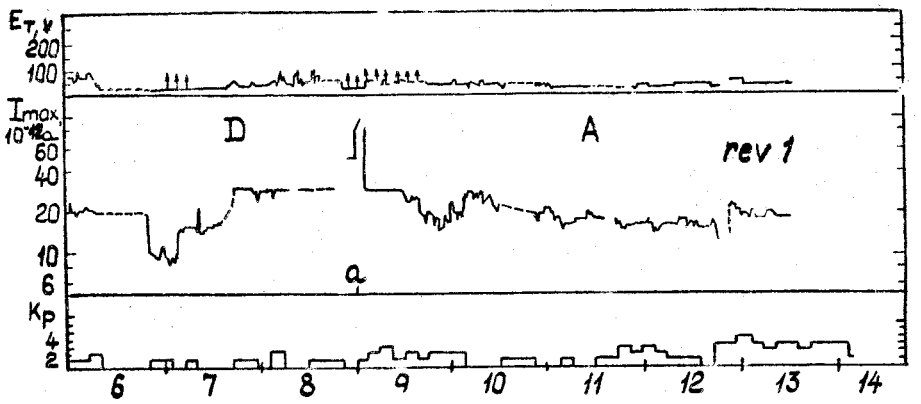

Mars -3 december 1971

Fig 6

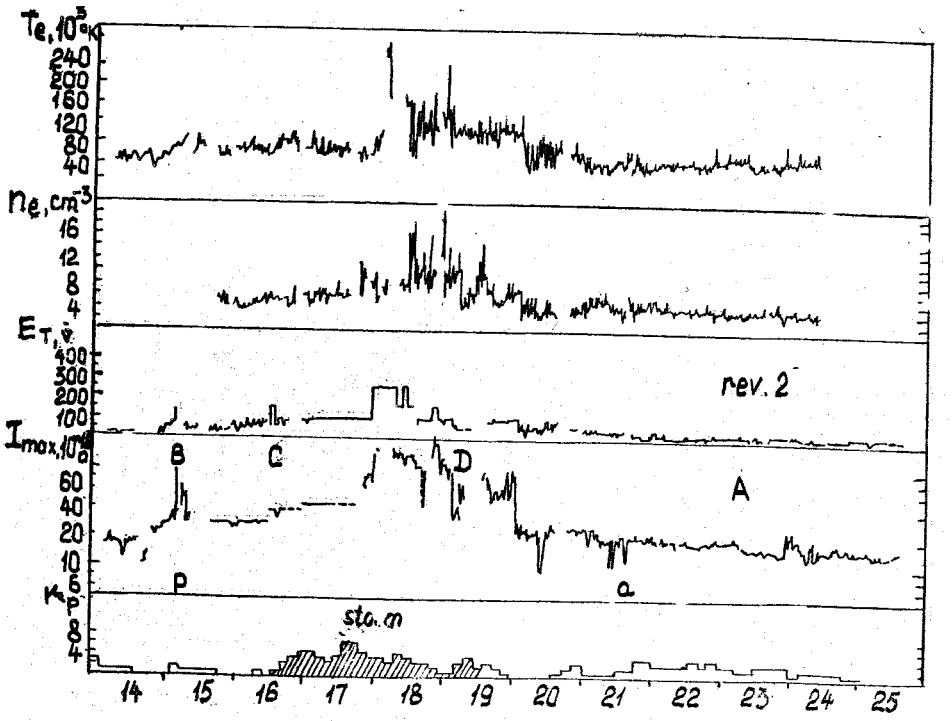

Mars-3 december 1971

Fig 7

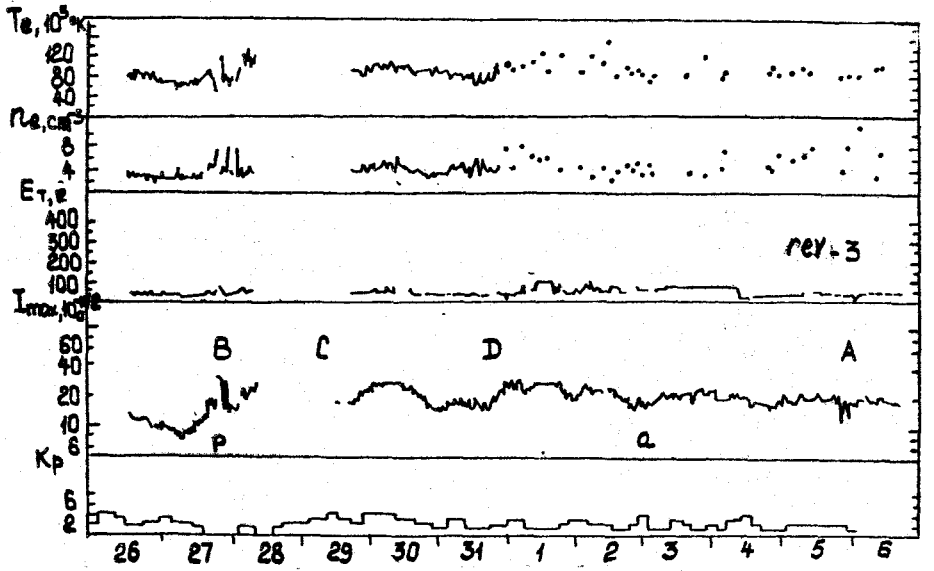
Te, 10⁵°K
120
80
40
ne, cm⁻³
8
4
Eт, в
400
300
200
100
rev. 3
Imax, 10⁻⁸a
60
40
20
10
6
B
C
D
A
P
a
Kp
6
2
26
27
28
29
30
31
1
2
3
4
5
6
december 1971
Mars 3
January 1972

Fig 8

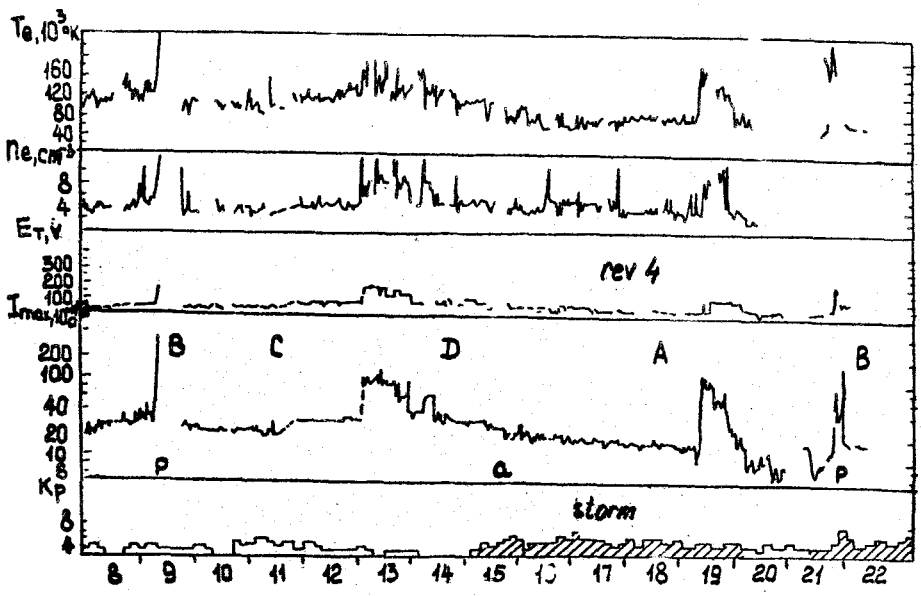
Te, 10³°K
160
120
80
40
ne, cm⁻³
8
4
Eт, в
500
200
100
rev 4
Imax, 10⁻⁸a
200
100
40
20
10
8
B
C
D
A
B
P
a
P
Kp
storm
8
4
8
9
10
11
12
13
14
15
16
17
18
19
20
21
22
Mars 3
January 1972

Fig 9

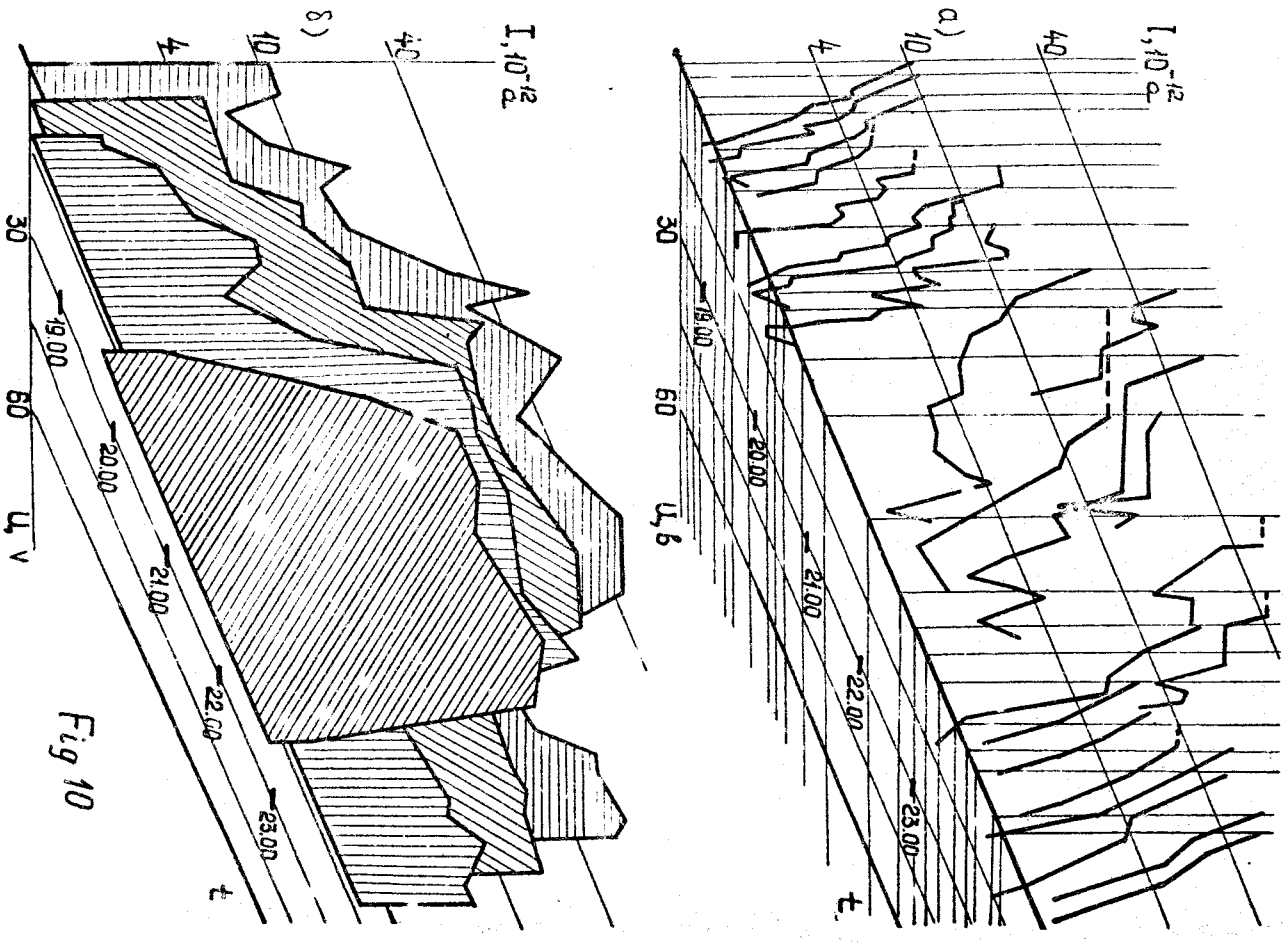

Fig 10

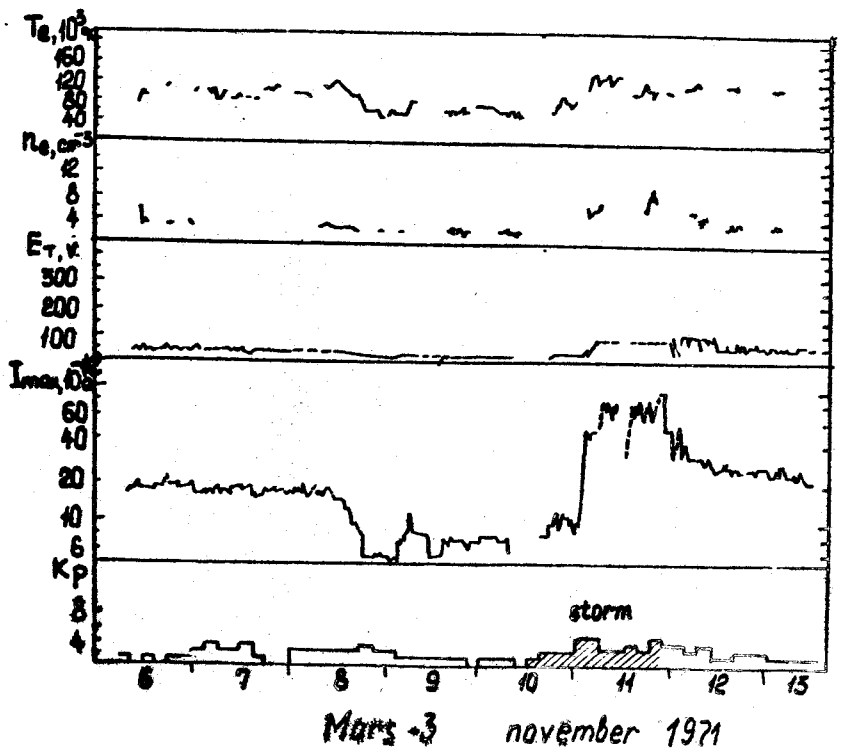

Mars-3 november 1971

Fig 11

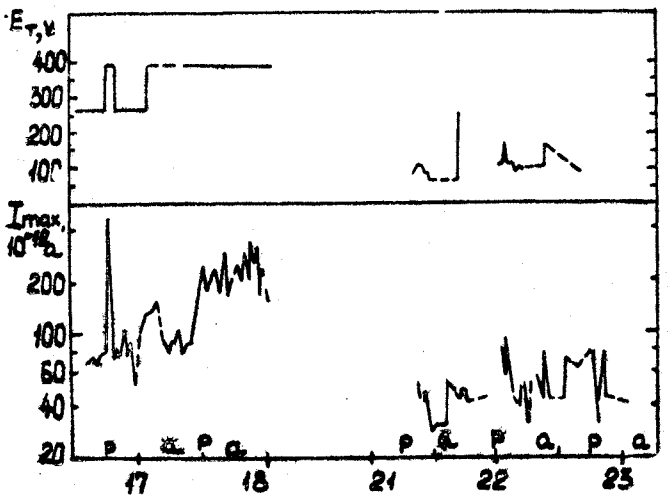

Fig 12

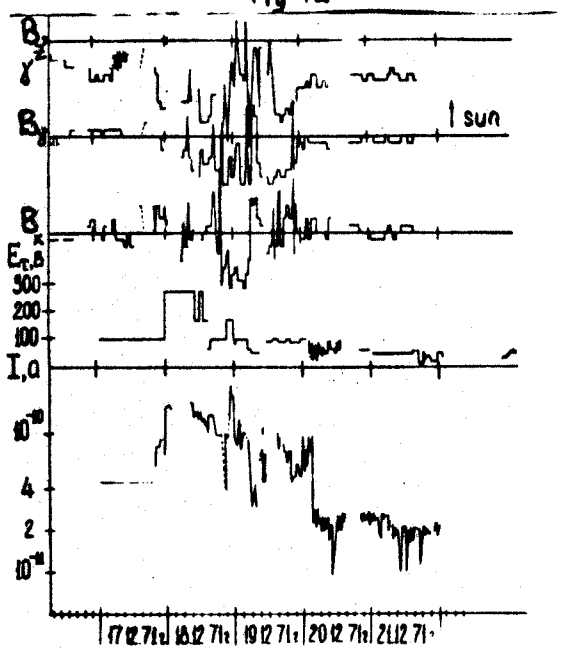

Fig 13

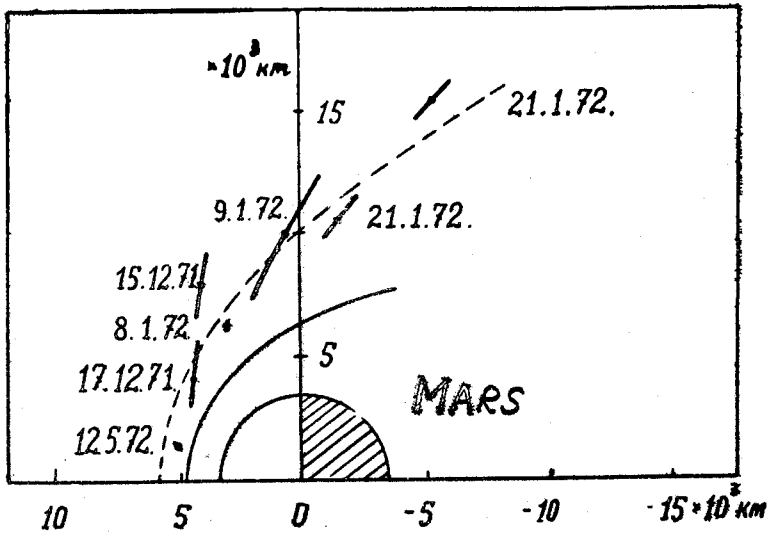

Fig 14

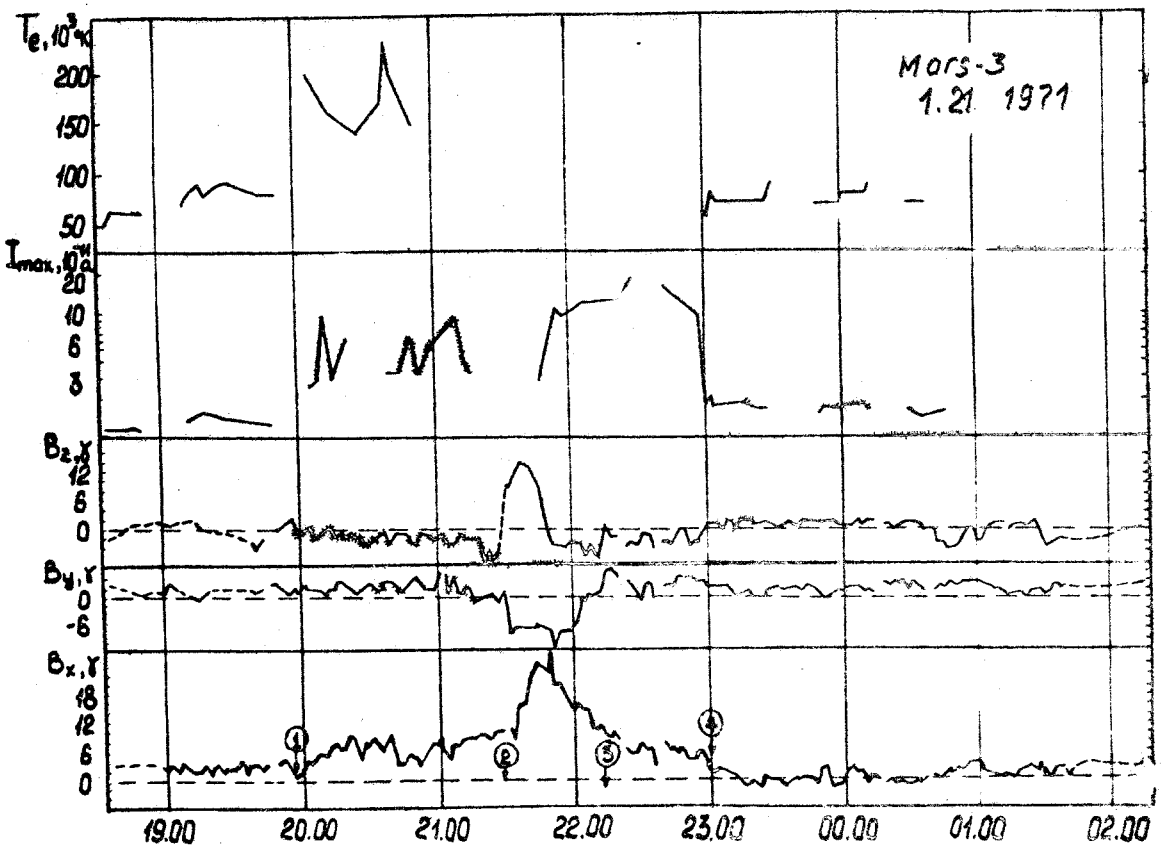
Mars-3
1.21 1971
$T_e, 10^3$ °K
200
150
100
50
$I_{max}, 10^{-11}$ a
20
10
6
3
B_z, γ
12
6
0
B_y, γ
0
-6
B_x, γ
18
12
6
0
1
2
3
4
19.00
20.00
21.00
22.00
23.00
00.00
01.00
02.00

Fig 15